International Journal of Heat and Mass Transfer 52 (2009) 5302–5308

Contents lists available at ScienceDirect

International Journal of Heat and Mass Transfer

journal homepage: www.elsevier.com/locate/ijhmt

Surface cooling based on the thermomagnetic convection: Numerical simulation and experiment

D. Zablotsky *, A. Mezulis, E. Blums

Institute of Physics, Latvian University, Miera Str. 32, Salaspils-1 LV-2169, Latvia

ARTICLE INFO

Article history:
Available online 26 August 2009

Keywords:
Ferrofluid
Thermomagnetic convection
Nusselt number
Thermosiphon
Cooling

ABSTRACT

In this paper we present the results of our numerical and experimental investigation of thermomagnetic convection in a temperature sensitive ferrofluid under the influence of strong non-uniform magnetic field. The convection is studied in a rectangular cell with permanent magnets attached to the cell walls. When the cell is heated from below, the observed intensification of heat transfer is significantly higher than that in the case of simple thermogravitational convection. The predictions of the numerical simulations are compared with the experimental results with good correspondence.

1. Introduction

Ferrofluids are stable colloidal suspensions of nanoscale ferromagnetic particles suspended in non-magnetic carrier, usually water or organic oil. The diameter of nanoparticles is ca. 10 nm. In order to prevent coagulation, the particles are sterically stabilized with layers of the surfactant. Due to their composition, such fluids exhibit superparamagnetic properties, which introduces into conventional transport processes an additional control parameter – the magnetic field, leading to appearance of new interesting effects.

The temperature dependence of magnetization causes appearance of a non-uniform body-force in differentially heated volume of ferrofluid, subjected to externally applied or internal magnetic field gradients [1]. The resulting convective motion – thermomagnetic convection – is in many ways similar to the thermogravitational one. In order to achieve high magnitude of driving force and intensive convection, special temperature-sensitive ferrofluids with high temperature dependence of magnetization as well as strong magnetic field gradients should be used.

The practical interest in thermomagnetic convection is motivated by its high potential for small scale cooling devices. The cooling of hot surfaces is an outstanding problem in a wide range of engineering and electronics applications. In most cases the classical gravity convection is unable to sustain adequate heat transfer efficiency in small scale setups or reduced gravity conditions, therefore forced convection is used in most technical applications. On the other hand, in strong magnetic fields the intensity of thermomagnetic convection can significantly exceed that of the pure thermogravitational. Compared to active setups currently employed in electronics, the relative simplicity of passive thermosiphon type ferrofluid cooling devices, based on self-regulating and self-sustaining nature of the thermomagnetic convection, and the absence of moving parts make it a highly interesting topic.

Since the prediction of Finlayson [2] of a novel convective instability in ferrofluids, leading to the thermomagnetic convection, a significant number of theoretical and experimental investigations have been performed in this area related to different geometries: Rayleigh–Bernard configuration, rectangular enclosure [3], cylinder [4–6], cube [7], partitioned cavity [8], etc. – and magnetic field configurations – homogenous distribution, constant field gradient [9], field of a line dipole [10] and others – confirming that the increase of convective heat transfer efficiency takes place under the applied magnetic field. Several attempts have been made to approach efficient cooling based on the ferrofluid convection both with magnetic coils and permanent magnets. Nakatsuka et al. [11] have investigated heat transfer characteristics of a heat pipe containing water-based magnetic fluid and measured 13% increase of heat transfer efficiency caused by non-uniform magnetic field. Yamaguchi et al. [12] numerically and experimentally investigated thermomagnetic convection in a rotation disk and came to a conclusion that vortexes impede convective heat transfer at high magnetic fields. Fumoto et al. [13] and most recently Li et al. [14,15] have thoroughly characterized the performance of a permanent magnet based miniature convection loop filled with temperature-sensitive ferrofluid, confirming the characteristic features of the thermomagnetic convection – stability and self regulation. For additional effect, in the latter work the Curie point of the ferrofluid was tuned to be within the operational temperature range.

* Corresponding author. Tel.: +371 67944664; fax: +371 67901214.
E-mail address: dmitrijs.zablockis@gmail.com (D. Zablotsky).

0017-9310/$ - see front matter © 2009 Elsevier Ltd. All rights reserved.
doi:10.1016/j.ijheatmasstransfer.2009.08.001

Nomenclature

c_p	heat capacity at constant pressure (J kg^{-1} K^{-1})
d	diameter of the cylindrical heater (m)
f	Kelvin's force (N)
g	gravitational acceleration (m s^{-2})
H	magnetic field intensity (H m^{-1})
h'	magnet shift (m)
I	current to the heater (A)
k_B	Boltzmann constant (=1.38 $\times$ 10^{-23} J K^{-1})
l	length of the heater (m)
L	characteristic distance (m)
m	magnetic moment of the ferroparticle (A m^2)
M	magnetization (A m^{-1})
M_{ref}	reference magnetization (A m^{-1})
M_S	saturation magnetization (A m^{-1})
Nu	Nusselt number
Pr	Prandl number
q	heat flux density (W m^{-2})
q_w	heat flux density through the heaters surface (W m^{-2})
Ra	gravity Rayleigh number
Re	Reynolds number
Rm	magnetic Rayleigh number
s_w	heater surface (m^2)
t	real time (s)
T	temperature (K)
T_{ref}	reference temperature (K)
u	vertical flow velocity (m s^{-1})
U	voltage on the heater (V)

Greek symbols

α	convective heat exchange coefficient (W/m^2 K)
β_m	pyromagnetic coefficient (K^{-1})
β_T	thermal expansion coefficient (K^{-1})
η	dynamic viscosity of the working liquid (N s m^{-2})
λ	thermal conductivity of the working liquid (W m^{-1} K^{-1})
μ_0	vacuum magnetic permeability (=4π $\times$ 10^{-7} H m^{-1})
ν	kinematic viscosity of the working liquid (m^2 s^{-1})
ρ	solvent density (kg m^{-3})
φ	particle volumetric concentration

The main challenge in designing a cooling device, based on the thermomagnetic convection, is achieving sufficiently high efficiencies of heat transfer, which requires special ferrofluids with high temperature sensitivity of magnetization. Prospective candidates for heat transfer applications are ferrofluids based on Mn–Zn nanoparticles, characterized by higher value of the pyromagnetic coefficient than widely used ferrite ones [16].

In this paper we report the results of our investigations of thermomagnetic convection in a rectangular convection cell filled with a temperature sensitive ferrofluid containing Mn–Zn nanoparticles. The aim of our research is to determine the intensity of convective motion and sustainable efficiency of the heat transfer due to thermomagnetic convection caused by sufficiently strong magnetic field. The experimental results are complemented by the numerical simulations.

2. Setup

The thermomagnetic convection has been investigated in a rectangular ferrofluid cell, made from plexiglass (Fig. 1) with dimensions 100 $\times$ 15 mm and 150 mm in height.

From both sides the cell is enclosed by strong permanent magnets 50 $\times$ 100 mm, begirded with a magnetic circuit. Two thin non-magnetic rigid ribs, positioned along the sides of the magnets, separate the central part of the cell. In order to reduce the heat loss from the large sidewalls, the cell is put in the plastic foam.

The working medium is a temperature sensitive ferrofluid DF-67K with Mn–Zn nanoparticles suspended in tetradecane. Magnetic granulometry measurements [5] at different temperatures have shown almost linear dependency of the magnetization in a wide temperature range between 20 and 250 °C and large value of the pyromagnetic coefficient. The main physical parameters of DF-67K and its solvent are summarized in Table 1. The temperature gradient, necessary for appearance of the thermomagnetic convection, is provided by the water reservoirs with constant temperature, placed at the upper and lower ends and separated from the surface of the cell with two semi-conductive 3 mm thick plates. The volume of ferrofluid is heated from the bottom and cooled from the top.

The applied magnetic field, provided by the permanent magnets, has been measured in the mid-plane of the convection cell along

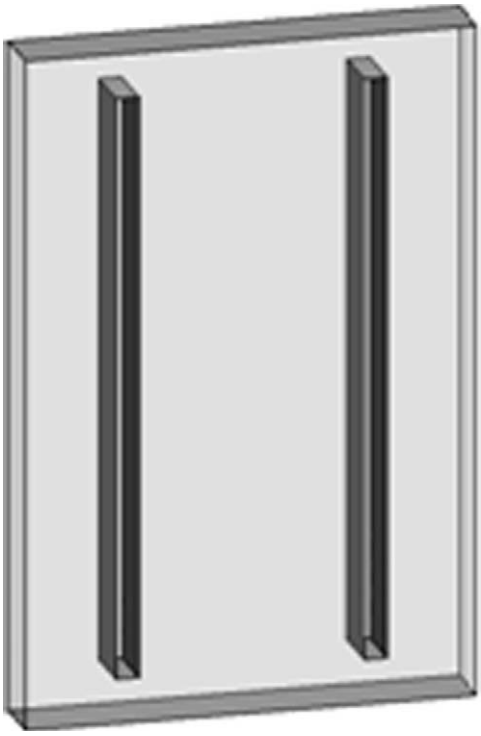

Fig. 1. Schematic view of the convection cell.

Table 1
Parameters of the ferrofluid DF-67 K.

Parameter	Value	Units
Solvent density	976	kg m^{-3}
Dynamic viscosity	0.006	Pa s
Specific heat capacity	2190	J kg^{-1} K^{-1}
Thermal expansion coefficient	9.33 $\times$ 10^{-4}	K^{-1}
Thermal conductivity	0.14	W m^{-1} K^{-1}
Particle diameter	~10	nm
Volumetric concentration	6	%
Saturation magnetization	1.2 $\times$ 10^6	A m^{-1}
Pyromagnetic coefficient	0.0028	K^{-1}

direction of the vertical axis of cell in three locations: at points A (at the center, $x = 0$ mm), B (along the side-edge of the magnet, $x = 25$ mm) and C ($x = 40$ mm). The results together with composed distribution of the magnetic field in the cell are shown in Fig. 2.

The strongest magnetic field in the cell volume between the poles is 640 kA m^{-1}, and its vertical gradient at the edges of poles is approximately 25,000 kA m^{-2}. The vertical separating ribs prevent the flow of fluid in lateral direction, effectively forming a thermomagnetic pump.

3. Numerical simulation

3.1. Governing equations

The external magnetic field in question is sufficiently strong to be considered constant, and all perturbations due to the ferrofluid motion can be neglected. The magnetic force, acting on the differentially heated non-conducting magnetic liquid, is described by Kelvin's body force:

$$\mathbf{f} = \mu_0(\mathbf{M}\nabla)\mathbf{H} \tag{1}$$

The magnetization of the ferrofluid is temperature-dependant. Introducing the linear equation of state:

$$M(T) = M_{ref}(1 - \beta_m(T - T_{ref})) \tag{2}$$

where $\beta_{ref} = \frac{1}{M_{ref}}\frac{\partial M}{\partial T}\big|_{T_{ref}}$ is the pyromagnetic coefficient. Reference magnetization has been calculated according to the single-parameter Langevin approximation:

$$M_{ref} = \varphi M_S \cdot L(\xi), \quad L(\xi) = \frac{1}{\tanh(\xi)} - \frac{1}{\xi}, \quad \xi = \frac{\mu_0 m_d H}{k_B T} \tag{3}$$

The flow of the magnetic fluid is governed by the incompressible Navier–Stokes equation, continuity equation and temperature equation without viscous dissipation. We have used the Boussinesq approximation and linear equation of state for the temperature dependence of density:

$$\rho(T) = \rho_{ref}(1 - \beta_T(T - T_{ref})) \tag{4}$$

Without the magnetic field, a convective motion in the cell can take place only due to buoyancy effects. In this regime the gravity Rayleigh number

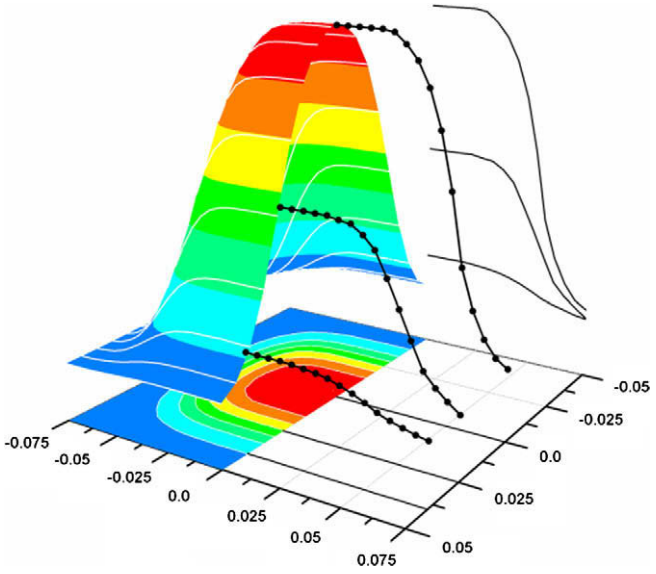

Fig. 2. Measured and reconstructed distribution of the magnetic field provided in the cell by permanent magnets.

$$Ra = \frac{\rho c_p L^3 \Delta T}{\eta\lambda}\beta_T \rho g \tag{5}$$

is much less than critical value for the onset of turbulence, therefore laminar convection takes place. This type of convection can be simulated directly within a reasonable timescale with conventional DNS approach.

By analogy with the thermogravitational convection, the magnetic Rayleigh number is introduced for the thermomagnetic convection

$$Rm = \frac{\rho c_p L^3 \Delta T}{\eta\lambda}\mu_0\beta_m M\nabla H \tag{6}$$

When a temperature sensitive ferrofluid is subjected to a strong magnetic field gradient, the magnetic Rayleigh number even for relatively small temperature differences proves to be orders of magnitude larger than the gravity Rayleigh number, and exceeds the critical threshold for the onset of turbulence. With the present setup at temperature difference 20 K a conservative estimation gives $Ra \approx 5 \times 10^6$ and $Rm \approx 5 \times 10^9$.

In order to simulate turbulent convection we have used RANS equation solver implemented in ANSYS CFX with SST k–w two-equation closure model.

The magnetic force was introduced via momentum source – this approach has been thoroughly validated by Snyder et al. [17].

Due to non-steady nature of thermal and thermomagnetic convection, transient simulations are required. All calculations were started from zero-velocity initial conditions and advanced with the time step varying from 0.1 to 50 ms. Transient averaging of velocity and temperature fields has been performed in order to distinguish convective patterns after averaged heat flux through the ferrofluid cell reached equilibrium. All parameters have been varied with the applied temperature difference 20 K, except when the temperature difference was changed itself.

3.2. Results

Calculated averaged velocity and temperature distributions in the ferrofluid cell at temperature difference over the full height of magnetic fluid volume $\Delta T = 20$ K, heated from below and cooled from above, are shown in Fig. 3a. The structure of the flow and position of the circulation areas are similar to the ones observed at lower Rayleigh and magnetic Rayleigh numbers in a laminar regime. The inner section of the cell between the areas of largest magnetic field gradient is occupied by two (considering symmetry) large recirculation areas, whereas smaller circulation areas are present at the lower end of the separating rib and in the upper corner of the cell.

The temperature distribution corresponding to this case is presented in Fig. 3b. The inner section of the convection cell between the separating ribs is occupied by a downgoing flow of slightly colder ferrofluid sucked in by the magnetic field. The warmer fluid, heated at the lower surface, is pushed out of the magnetic field to the outer section of the cell, where it rises along the sidewall due to buoyancy forces.

The averaged velocity profile in the middle of the cell between the separating ribs is shown in Fig. 4. The length-average absolute velocity across the profile is approximately 21 mm s^{-1}. This value will be compared with the experimental results of hot-wire velocimetry.

Another interesting case is when the applied temperature gradient is oriented upwards. In this case the ferrofluid in the convection cell is heated from the top and cooled from the bottom, and the thermomagnetic convection is not aided by buoyancy. Calculated averaged streamlines with the temperature difference 20 K are shown in Fig. 5a, and the corresponding temperature contour

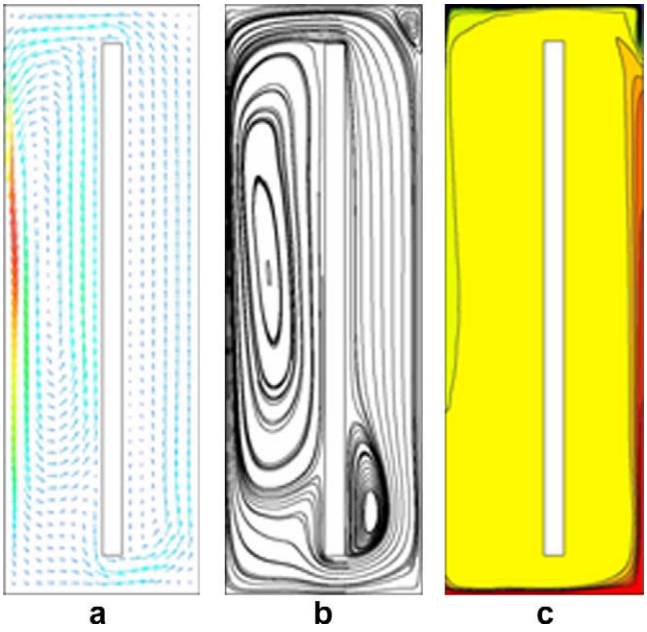

Fig. 3. Calculated averaged velocity and temperature distributions with temperature difference $\Delta T = 20$ K: (a) averaged velocity vectors (b) streamlines (c) temperature distribution, heated from below.

plot in Fig. 5b. The structure of the flow is very similar to the case of temperature gradient oriented downwards, which means that the characteristic features of the flow are determined actually by the magnetic field, and the thermogravitational convection plays a secondary role, as it follows from the estimated ratio of thermogravitational and thermomagnetic Rayleigh numbers.

Additional calculations at other temperature differences have been carried out. Increasing the applied temperature difference between the bottom and top surfaces of the ferrofluid cell to 40 or 80 K splits and suppresses the circulation areas in the inner section of the cell and expands the one near the lower end of the separating rib (Fig. 6).

The temperature profiles in these cases are very similar to the ones at 20 K and are not shown.

The heat transfer efficiency of convection can be characterized by the Nusselt number as a ratio of heat flux through the ferrofluid cell due to convective motion to the one due to heat conduction. We use the relative Nusselt number Nu/Nu_0 instead, defined as a ratio of heat flux through the cell due to thermomagnetic convection to the heat flux due to the thermogravitational convection only, averaged over sufficient time interval. The dependence of

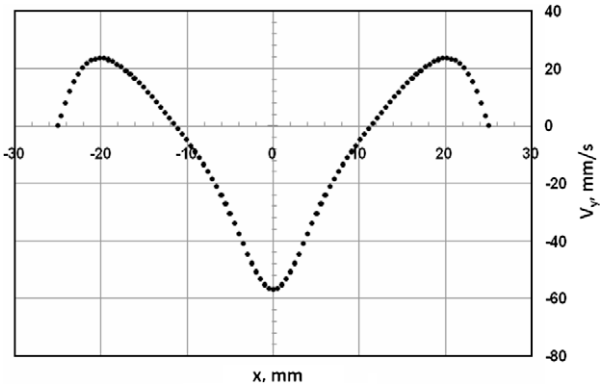

Fig. 4. Averaged velocity profile along the midline of the cell between the separating ribs.

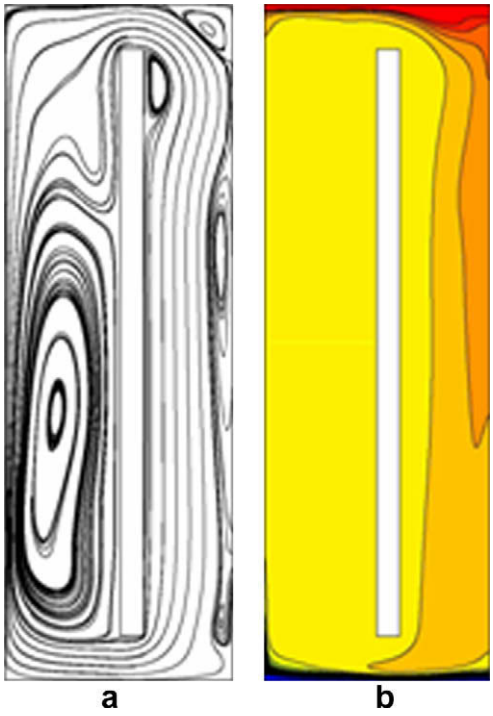

Fig. 5. Calculated averaged velocity and temperature distributions for temperature difference $\Delta T = 20$ K: (a) streamlines (b) temperature distribution, heated from above.

the relative Nusselt number on the applied temperature difference is shown in Fig. 7a.

The heat transfer efficiency slightly decreases with increasing the heat load on the ferrofluid cell. Such an effect may exist due to the change of flow regime at higher applied temperature difference: under action of the magnetic field a transition to the turbulence takes place, leading to different scaling law.

In order to determine the optimal position of the magnetic poles, additional series of calculations has been performed with different magnetic field shifts along the axis of the cell (y-axis), relative to the symmetrical placement. The dependence of the relative Nusselt number on the position of the magnets h' is shown in Fig. 7b. The heat transfer efficiency is significantly increased if the ferrofluid is heated in the area of maximum field gradient. The maximum intensification of convective heat transfer in this series, when the magnet is shifted 20 mm downwards, is approximately 2 times. Further shifting of the magnetic field was prevented by the experimental setup.

4. Experiment

Experimental setup is shown schematically in Fig. 8. In experiments the temperature gradient in semi-conductive 3 mm thick plates, which are placed between convection cell ends and warm/cold water reservoirs, is measured. From these measurements the heat flux density q through the plates is calculated, which leads to obtaining the convective heat exchange coefficient between working liquid and the plates in upper and lower ends of the cell: $\alpha = q/\Delta T$. Experimental setup allows the shift of magnets up and down along the convection cell to search for the best intensification of magnetoconvection by changing heating/cooling ratio at the edges of the magnets.

Experimental results are collected with the aim to compare them with Fig. 7a and b. The only dissimilarity is using the heat exchange coefficient α, which seems to be preferable by its simple measuring technique, instead of Nu.

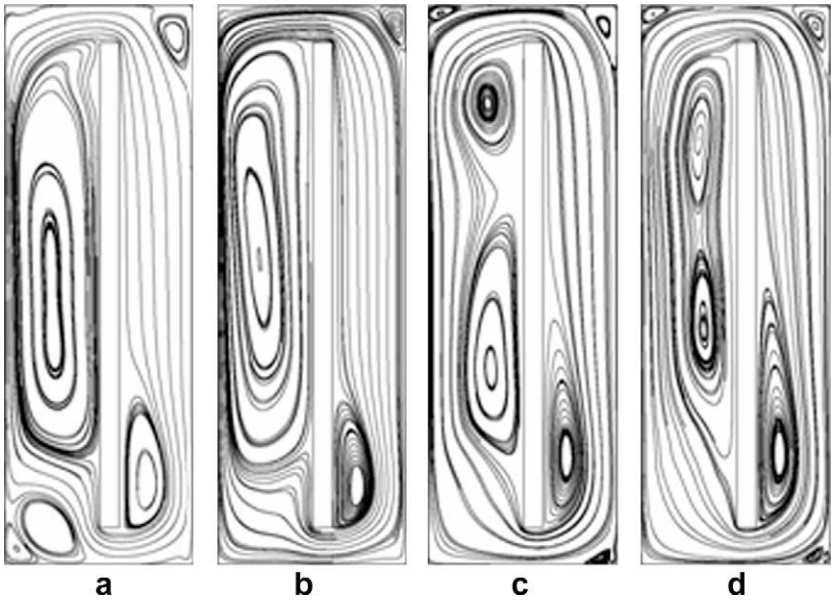

Fig. 6. Calculated averaged velocity: (a) streamlines at $\Delta T = 10$ K (b) streamlines at $\Delta T = 20$ K (c) streamlines at $\Delta T = 40$ K (d) streamlines at $\Delta T = 80$ K, heated from below.

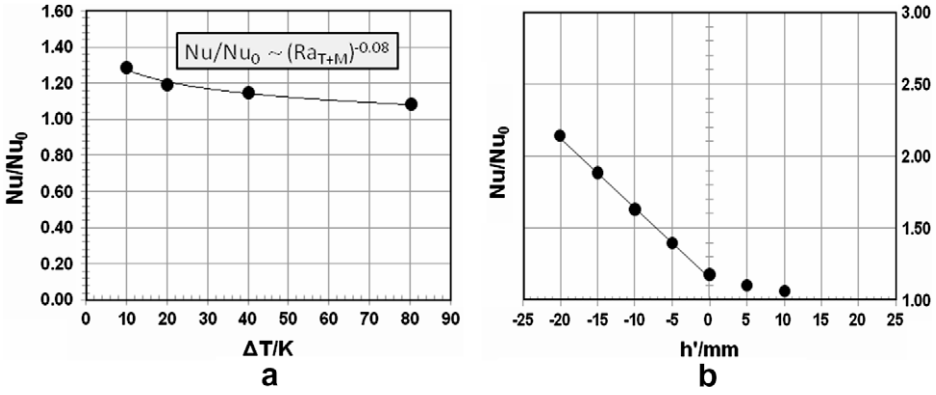

Fig. 7. Intensification of convective heat transfer through the cell (a) at various temperature differences, $h' = 0$ (b) shifted positions of the magnetic field, $\Delta T = 20$ K.

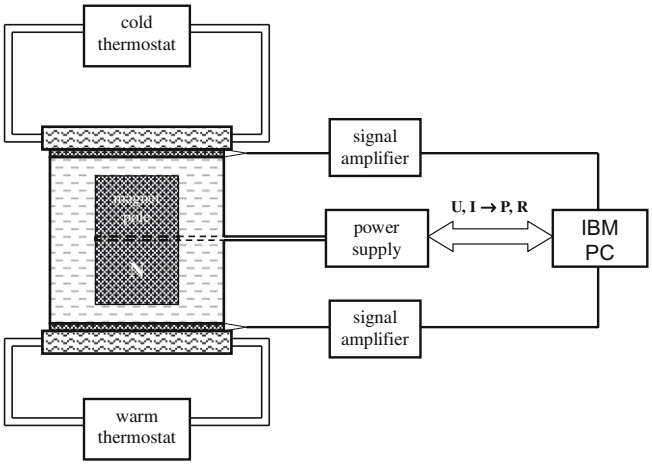

Fig. 8. Experimental setup.

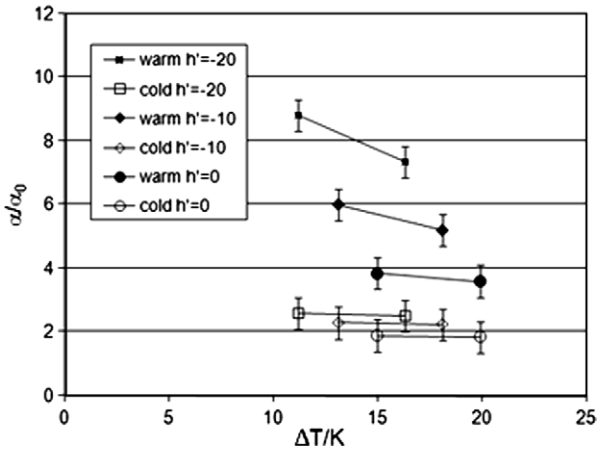

Fig. 9. Measurements of relative heat exchange coefficient α/α_0 vs. the temperature difference ΔT with three magnet positions h'.

Fig. 9 shows the relative heat exchange coefficient α/α_0 as a function of ΔT with three magnet positions. The temperature difference ΔT varies with the magnet shift h' because the experiments are performed at certain temperature difference between the heater and the cooler. Obviously, one must subtract the temperature differences on the semi-conductive plates ($\sim$10 K) to obtain ΔT.

In order to save hermetism of the convection cell at acting thermal expansion stresses, in experiments the temperature difference is varied only in a short range, 10 K. It makes no sense to try to obtain curving of a very slight slope within inherent experimental accuracy, therefore taken dependences are linearized.

The difference of the heat exchange at warm and cold ends of the cell can be explained by heat loss through the quite large cell sidewalls. Indeed, the temperature of the laboratory room 15 °C is much closer to that of the cold end 10 °C. During experiments the cell has been put into plastic foam, but as a matter of fact it avoided this effect only partially.

By analogy with Fig. 7b in the theoretical part, Fig. 10 shows determined relative heat exchange coefficient α/α_0 vs. the magnet shift h' at fixed temperature difference $\Delta T = 20$ K.

In Fig. 10 it is clearly seen how strong the heat exchange coefficient depends on the magnet position. More efficient turns to be lower placement of the magnets $h' < 0$, i.e. the magnetic field nearer to the warm end (for the present setup the range of magnet shift is ±20 mm). We get maximal value of the heat exchange coefficient $\alpha_{max} = 47$ W/m^2 K at the warm end, when the magnets are maximally shifted downwards. In the stationary state of this experiment the heat flux density on the warm (i.e. cooled) surface reaches 750 W m^{-2}.

Additional series of measurements regard the small cylindrical heater of diameter $d = 4$ mm, which is placed horizontally between the separating ribs in the middle of the cell. The length of the heater, as well as the distance between the ribs $l = 50$ mm matches exactly that of the magnet, see Fig. 8. The voltage and the current of the heater are measured with a high accuracy. From these measurements the ohmic resistance of the heater is calculated to find out the temperature of the heater body. Also the density of dissipated power through the heater surface can be easily calculated:

$$q_w = \frac{UI}{s_w}. \tag{7}$$

The governing equation of the laminar flow allows to calculate vertical flow velocity u of the working liquid around the cylindrical heater [18]:

$$Nu = 0.664\sqrt{Re}\sqrt[3]{Pr}, \tag{8}$$

where the Reynolds number $Re = \pi\, du/2\nu$ includes searched velocity u, and the Prandl number $Pr = \rho c_p \nu/\lambda$. In contradistinction to the relative Nusselt number, used in the theoretical part of the paper, Eq. (8) considers the conventional Nusselt number $Nu = q_w d/\lambda \Delta T_w$, which is calculated from experimental data U, I, ΔT_w by Eq. (7). Note that ΔT_w is the temperature difference between the surface of the heater and magnetic fluid at the middle of volume.

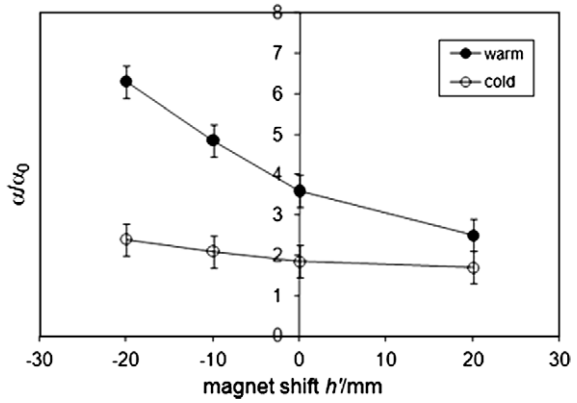

Fig. 10. Dependence of relative heat exchange coefficient α/α_0 on magnet shift: $h' > 0$ means the magnet shift upwards, $h' = 0$ is the central magnet position (as shown in Fig. 8).

Vertical flow velocity measurements have been carried out at zero and non-zero magnetic field. Obtained absolute Nusselt number turns out to be rather independent from dissipated electric power of the heater 5, 10 and 15 W. Obtained results are shown in Table 2. The second column of the Table 2 displays velocity of the working liquid around the heater, calculated by Eq. (8). For the corrected main velocity (the third column) the diminution of cross-section of the cell due to the heater body is taken into account: from the flow continuity $s \cdot u = const$ one should reduce the velocity away from the heater by a proportion of corresponding gap widths (mm): (15 − 4)/15.

5. Discussion

The main subject of discussion is the accordance between results of numerical simulation and experimental work, which turns out to be rather good. Let us compare numerically simulated Fig. 7a and b with experimentally obtained Figs. 9 and 10. The effect that lower temperature difference gives more magnetic intensification related to zero field experiments, is shown in Fig. 7a with Nu/Nu_0 as well as in Fig. 9 with α/α_0 (the case $h' = 0$). For the case $h' = 0$ Fig. 7 gives the increment of intensification of ∼4% with respect to changing ΔT from 20 to 15 K. From experimental results (Fig. 9) one obtain ∼5% at the warm end and 1–2% at the cold end. These results seem to be correct by taking into account nonsymmetrical heat loss through the sidewalls of the cell.

Second point is to compare Fig. 7b with Fig. 10. Numerical simulation gives the relation Nu/Nu_0 vs. the magnet shift h' (mm) to be quite constant within the range $-20 < h' < 0$ and equal to -0.05 mm^{-1}. Experiment provides with α/α_0 vs. the magnet shift h' that also is rather constant from −20 mm up to at least 0 mm, and farther up to 20 mm only a little less. Paying attention to the range −20 to 0 mm, experimentally obtained slopes α/α_0 vs. h' (mm) are -0.13 mm^{-1} at the warm end and -0.03 mm^{-1} at the cold end. As in the first comparison, the numerical estimation is between experimental ones at both ends. Although, quantitatively in the experiment the warm end exhibits 2–3 times larger sensitivity to the magnet shift than the numerical estimation. The main reason may be that theoretical model deals with simplified configuration of the magnetic field, moreover, β_T is ignored in the magnetic Rayleigh number Rm. That causes a larger discrepancy with taking the magnetic field nearer to the heater.

At the end, the value of averaged vertical velocity can be compared. The result of numerical simulation is 21 mm s^{-1} with the magnet position $h' = 0$ (Fig. 4). Table 2 gives for that case the corrected main velocity 20 ± 2 mm s^{-1}. Perfect accordance in such a complicated both simulation and experiment might be taken partly as an occasion, but as a matter of fact, the accordance in this point is primely proved.

6. Conclusions

In a convection cell with attached permanent magnets the thermomagnetic convection may exceed that of thermogravitational

Table 2
Obtained averaged between the separating ribs vertical flow velocity (estimated accuracy ±2 mm s^{-1}).

Experimental conditions	Velocity along the heater (mm s^{-1})	Corrected main velocity (mm s^{-1})
Zero-field experiment	12	9
Magnet position $h' = 0$ mm	27	20
Magnet position $h' = -20$ mm	38	28

many times. Efficiency of the thermomagnetic convection depends on placement of magnets with respect to warm and cold ends of the cell. Maximal thermomagnetic intensification is achieved when magnets are placed as near as possible to the warm (cooled) end.

Comparision between numerically simulated and experimentally obtained results proves to be quite successful. Results are compared in three aspects: magnetic intensification as dependent on the temperature difference, on the magnet shift, and averaged vertical flow velocity. The accordance varies from perfect to 2–3 times quantitatively. In fact, the accordance between derivatives of magnetic intensification on the temperature difference and on the magnet shift cannot be given precisely. Due to technical reasons the experiment provides short range of changing parameters, so the accuracy of obtaining derivatives is of the same order as comparison with the numerical results.

The applying of surface cooling based on the thermomagnetic convection in technical use is under the question. Reached with the present setup the cooling effect of 0.075 W cm^{-2} seems to meet only low technical demands. The present work proves the finding of Rosensweig [19] that a significant augment of the cooling intensity by thermomagnetic convection can be obtained only in a case if the heat source is located into the region of a maximal magnetic field intensity, when the efficiency of power generation cycle reaches its maximum.

References

[1] E. Blums, A. Cebers, M.M. Maiorov, Magnetic Fluids, Walter de Gryuter, Berlin, 1997.
[2] B.A. Finlayson, Convective instability of ferromagnetic fluids, J. Fluid Mech. 40 (4) (1970) 753.
[3] M.S. Krakov, I.V. Nikiforov, To the influence of uniform magnetic field on thermomagnetic convection in square cavity, J. Magn. Magn. Mater. 252 (2002) 209–211.
[4] A. Lange, Thermal convection of magnetic fluids in a cylindrical geometry, J. Magn. Magn. Mater. 252 (2002) 194–196.
[5] E. Blums, A. Mezulis, G. Kronkalns, Magnetoconvective heat transfer from a cylinder under the influence of a nonuniform magnetic field, J. Phys.: Condens. Matter 20 (20) (2008).
[6] D. Zablockis, V. Frishfelds, E. Blums, Numerical investigation of thermomagnetic convection in a heated cylinder under the magnetic field of a solenoid, J. Phys.: Condens. Matter 20 (20) (2008).
[7] M.S. Krakov, I.V. Nikiforov, A.G. Reks, Influence of the uniform magnetic field on natural convection in cubic enclosure: experiment and numerical simulation, J. Magn. Magn. Mater. 289 (2005) 272–274.
[8] H. Yamaguchi, Z. Zhang, S. Shuchi, K. Shimada, Heat transfer characteristics of magnetic fluid in a partitioned rectangular box, J. Magn. Magn. Mater. 252 (2002) 203–205.
[9] T. Sawada, H. Kikura, T. Tanahashi, Visualization of wall temperature distribution caused by natural convection of magnetic fluids in a cubic enclosure, Int. J. Appl. Electromagn. Mater. 4 (4) (1994) 329–335.
[10] R. Ganguly, S. Sen, I.K. Puri, Heat transfer augmentation using a magnetic fluid under the influence of a line dipole, J. Magn. Magn. Mater. 271 (1) (2004) 63–73.
[11] K. Nakatsuka, B. Jeyadevan, S. Neveu, H. Koganezawa, The magnetic fluid for heat transfer applications, J. Magn. Magn. Mater. 252 (2002) 360–362.
[12] H. Yamaguchi, A. Sumiji, S. Shuchi, T. Yonemura, Characteristics of thermomagnetic driven motor using magnetic fluid, J. Magn. Magn. Mater. 272-276 (3) (2004) 2362–2364.
[13] F. Koji, Y. Hideaki, I. Masahiro, A mini heat transport device based on thermosensitive magnetic fluid, Nanoscale Microscale Thermophys. Eng. 11 (1) (2007) 201–210.
[14] Q. Li, W. Lian, H. Sun, Y. Xuan, Investigation on operational characteristics of a miniature automatic cooling device, Int. J. Heat Mass Transfer 51 (21) (2008) 5033–5039.
[15] W. Lian, Y. Xuan, Q. Li, Characterization of miniature automatic energy transport devices based on the thermomagnetic effect, Energy Convers. Manage. 50 (1) (2009) 35–42.
[16] M. Maiorov, E. Blums, H. Hanson, C. Johanson, High field magnetization of the colloidal Mn–Zn ferrite, J. Magn. Magn. Mater. 85 (1990) 129–132.
[17] S.M. Snyder, T. Cader, B.A. Finlayson, Finite element model of magnetoconvection of a ferrofluid, J. Magn. Magn. Mater. 262 (2) (2003) 269–279.
[18] V.P. Isachenko, V.A. Osipova, A.S. Sukomel, Teploperedacha (in Russian), Energiya, Moskva-Leningrad, 1965.
[19] R.E. Rosensweig, Ferrohydrodynamics, Cambridge University Press, Cambridge, MA, 1985. 344 pp..